

A Boundary Element - Response Matrix method for 3D neutron diffusion and transport problems

V.Giusti¹, B.Montagnini²

¹Department of Civil and Industrial Engineering, Pisa University, Largo Lucio Lazzarino 2, I-56126, Pisa, ITALY, v.giusti@ing.unipi.it

²Department of Civil and Industrial Engineering, Pisa University, Largo Lucio Lazzarino 2, I-56126, Pisa, ITALY, b.montagnini@ing.unipi.it

Keywords: Response matrix, Neutron diffusion, Neutron transport, 3D criticality problems

Abstract. An application of a 3D Boundary Element Method (BEM) coupled with the Response Matrix (RM) technique to solve neutron diffusion and transport equations for multi-region domains is presented. The discussion is here limited to steady state problems, in which the neutrons have a wide energy spectrum, which leads to systems of several diffusion or transport equations. Moreover, the number of regions with different physical constants can be very large. The boundary integral equations concerning each region are solved via a polynomial moment expansion and the multi-fold integrals there involved are reduced to single or double integrals, taking advantage of suitable recurrence formulas. The usual unknowns (the boundary particle density and its normal derivative) are here replaced by the partial currents entering or leaving each cell. The intuitive physical meaning of such quantities facilitates the application of the response matrix technique. Only eigenvalue (criticality) problems will be here considered. As it regards the transport equation, the use of the so called Simplified Spherical Harmonics method allows, through suitable approximations, to cast the problem into a system of differential elliptic equations of the diffusion type, which can still be solved by BEM.

Introduction. The computational methods based on the Boundary Element Method (BEM) here presented have been devised for the calculations of the nuclear reactor cores, a subject which is almost a taboo in Italy but not in other developed or emerging countries (e.g. France, Russia or China), also as a valid option to contrast the persisting (and even increasing) use of coal, oil and gas.

An exhaustive collection of historical references on the application of BEM to neutronic problems is outside the aim of this paper. Thus we limit ourselves to list some relevant works. The first paper, with a rather complete account of the basic theory, goes back to Koskinen [1]. At the beginning of eighties, further developments [2, 3] gave a strong impulse to BEM, owing to the introduction of the Multiple Reciprocity Method (MRM) [4, 5, 6, 7, 8, 9, 10]. Despite of its elegance, the MRM method has not completely ruled out other classical methods for systems of second order partial differential equations (also pointed out in some of the aforementioned papers), i.e. the diagonalization method and the direct domain (volume) integration. A second step was represented by the decoupling of the global problem into two levels [11, 12, 13, 14]. Another approach will be sketched here below [15, 16, 17].

This paper aims to give a quick account of BEM as applied to practical reactor calculations where the neutron traffic, $\phi(\mathbf{r})$, (i.e. neutron density times neutron speed) commonly referred to as neutron flux, has to be determined in the reactor core under steady state conditions.

The simplest model is thus based on a system of diffusion equations, one for each speed (or energy) group into which the neutron population can be divided:

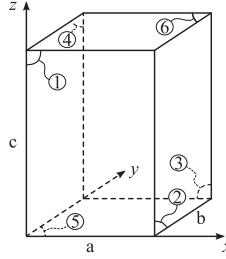


Figure 1: Face numbering on the rectangular node.

$$\begin{aligned} \nabla \cdot D_g(\mathbf{r}) \nabla \phi_g(\mathbf{r}) - \Sigma_{a,g} \phi_g(\mathbf{r}) + \sum_{g'=1}^G \Sigma_{s,gg'} \phi_{g'}(\mathbf{r}) \\ + \frac{\chi_g}{k} \sum_{g'=1}^G \nu_{g'} \Sigma_{f,g'} \phi_{g'}(\mathbf{r}) \quad (g = 1, \dots, G) \end{aligned} \quad (1)$$

where D_g , $\Sigma_{a,g}$, $\Sigma_{s,gg'}$ and $\nu_g \Sigma_{f,g}$ are, respectively, the diffusion coefficient, the absorption cross section, the scattering cross section from group g' to group g and the fission cross section times ν_g , the number of secondary neutrons emitted by this process whose energy falls inside the group g . Finally, χ_g is the fraction of secondary neutrons whose energy is within the group g , while k represents the multiplication constant, which plays the role of eigenvalue of the equation system, and it is equal to one under steady state (critical) conditions.

The commonly used conditions on the reactor boundary are vanishing conditions for each ϕ_g .

The main difficulties as regards the application of BEM to such problems are: (i) the problem domain is, in general, a 3D domain, (ii) the number of equations, G , is rather large, (iii) the reactor core is physically divided into homogeneous (i.e. uniform) regions (or made homogeneous through suitable averaging procedures), but such regions might be thousands.

The lucky circumstance is that the regions or 'cells' (as we will refer to them from now on) to be considered during the calculation have a rather simple shape: usually right prisms with a rectangular, hexagonal or triangular base, which are arranged accordingly to a regular lattice. As pointed out above the calculation procedure can be divided into two steps or levels:

- the first level: one considers the neutrons entering each cell from the boundary, which is accomplished by giving ϕ_g or its normal derivative, $\partial\phi_g/\partial n$. Making use of BEM it is then possible to determine those neutrons which leave the cell and will therefore be considered as entering the adjacent ones;

- the second level: on the basis of the ingoing and outgoing particles, an iterative procedure is established in order to determine the neutron distribution over the global reactor system as well as the multiplication constant.

The first level: solution of the diffusion equation system for a single cell. Let us consider for simplicity a lattice cell, V , with the shape of a prism with rectangular base and sides a , b , and c and homogeneous physical properties (see Fig.1).

Equation system (1) can be rewritten in compact form

$$\Delta\phi + \mathbf{Q}\phi = 0 \quad (2)$$

(the eigenvalue k is embedded in the matrix \mathbf{Q} , in which all the physical properties are contained, and is provisionally understood). Through a diagonalization of \mathbf{Q} the system is reduced to the form

$$\Delta\psi + \Lambda\psi = 0 \quad (\Xi^{-1}\mathbf{Q}\Xi = \Lambda) \quad (3)$$

where the equations are now uncoupled. The eigenvalues λ_h are in general complex. However, in the simplest case, $\lambda_h = -\gamma_h^2$ (with γ_h real and positive) and the fundamental solution of equation (3) is a familiar one, namely

$$\tilde{\psi}_h(\mathbf{r}, \mathbf{r}') = \frac{\exp(-\gamma_h |\mathbf{r} - \mathbf{r}'|)}{4\pi |\mathbf{r} - \mathbf{r}'|}. \quad (4)$$

The usual procedure of the BEM direct method allows to obtain the following integral form

$$c(\mathbf{r}) \psi_h(\mathbf{r}) + \int_S \left[\frac{\partial \tilde{\psi}_h}{\partial n'_S}(\mathbf{r}, \mathbf{r}'_S) \psi(\mathbf{r}'_S) - \tilde{\psi}_h(\mathbf{r}, \mathbf{r}'_S) \frac{\partial \psi_h}{\partial n'_S}(\mathbf{r}'_S) \right] dS' \quad (5)$$

($c(\mathbf{r})$ = characteristic function of the V cell). Applying once again the matrices Ξ and Ξ^{-1} we go back to the physical unknowns.

$$c(\mathbf{r}) \phi_g(\mathbf{r}) + \sum_{g'=1}^G \int_S \left(\frac{\partial \tilde{\phi}_{gg'}}{\partial n'_S}(\mathbf{r}, \mathbf{r}'_S) \phi_g(\mathbf{r}'_S) - \tilde{\phi}_{gg'}(\mathbf{r}, \mathbf{r}'_S) \frac{\partial \phi_{g'}}{\partial n'_S}(\mathbf{r}'_S) \right) dS' = 0 \quad (6)$$

$(g = 1, \dots, G),$

where \mathbf{r} is any point of V , while \mathbf{r}_S denotes a boundary point. Taking \mathbf{r} on the boundary, too, one obtains the set of the Boundary Integral Equations (BIE) that replaces the differential system (1) for a single cell:

$$c(\mathbf{r}_S) \phi_g(\mathbf{r}_S) + \sum_{g'=1}^G \int_S \left(\frac{\partial \tilde{\phi}_{gg'}}{\partial n'_S}(\mathbf{r}_S, \mathbf{r}'_S) \phi_g(\mathbf{r}'_S) - \tilde{\phi}_{gg'}(\mathbf{r}_S, \mathbf{r}'_S) \frac{\partial \phi_{g'}}{\partial n'_S}(\mathbf{r}'_S) \right) dS' = 0 \quad (7)$$

$(g = 1, \dots, G).$

A rearrangement of the unknowns, suggested by the physics of the diffusion process, is useful. It is related to the notion of outward and inward partial currents at a point of the boundary surface S , namely:

$$J_g^\pm(\mathbf{r}_S) = \frac{1}{4} \phi_g(\mathbf{r}_S) \mp \frac{1}{2} D_g \frac{\partial \phi_g}{\partial n_S}(\mathbf{r}_S). \quad (8)$$

With these variables, system (7) is replaced by the following one

$$\begin{aligned} \frac{c(\mathbf{r}_S)}{2} J_g^+(\mathbf{r}_S) + \sum_{g'=1}^G \int_S \tilde{J}_{gg'}^+(\mathbf{r}_S, \mathbf{r}'_S) J_{g'}^+(\mathbf{r}'_S) dS' &= -\frac{c(\mathbf{r}_S)}{2} J_g^-(\mathbf{r}_S) \\ &+ \sum_{g'=1}^G \int_S \tilde{J}_{gg'}^-(\mathbf{r}_S, \mathbf{r}'_S) J_{g'}^-(\mathbf{r}'_S) dS' \quad (g = 1, \dots, G). \end{aligned} \quad (9)$$

Let the ingoing currents J_g^- be known (so that the *r.h.s* is known). Then the response of the cell in terms of the outgoing currents J_g^+ will be determined by solving the BIE's with the kernels $J_{gg'}^+(\mathbf{r}_S, \mathbf{r}'_S)$. The second or global level, in which all the cells are connected all together, can be then based on the following iteration steps

$$\begin{aligned} \frac{c(\mathbf{r}_S)}{2} J_g^{+t+1}(\mathbf{r}_S) + \sum_{g'=1}^G \int_S \tilde{J}_{gg'}^+(\mathbf{r}_S, \mathbf{r}'_S)^{t+1} J_{g'}^+(\mathbf{r}'_S) dS' &= -\frac{c(\mathbf{r}_S)}{2} J_g^-(\mathbf{r}_S) \\ &+ \sum_{g'=1}^G \int_S \tilde{J}_{gg'}^-(\mathbf{r}_S, \mathbf{r}'_S)^t J_{g'}^-(\mathbf{r}'_S) dS' \quad (g = 1, \dots, G). \end{aligned} \quad (10)$$

Let us return, however, to the single cell problem. To perform the numerical solution, the inward and outward partial currents are expanded into polynomials $w_{s,mn}(\mathbf{r})$ over the s_M faces ($s_M = 6$ in our case) of the parallelepiped V :

$$J_g^\pm(\mathbf{r}_S) \simeq \sum_{s=1}^{s_M} \sum_{m=0}^{m_M} \sum_{n=0}^{n_M} J_{g,smn}^\pm w_{s,mn}(\mathbf{r}_S) \quad (11)$$

and similar expressions are adopted for the kernels $\tilde{J}_{gg'}^\pm(\mathbf{r}_S, \mathbf{r}'_S)$.

The BIE are then replaced by a linear system as follows

$$\begin{aligned} \frac{1}{4} J_{g,smn}^+ + \sum_{g'=1}^G \sum_{s'=1}^{s_M} \sum_{m'=0}^{m_M} \sum_{n'=0}^{n_M} \tilde{J}_{gg',ss'mm'nn'}^+ J_{g',s'm'n'}^+ = \\ - \frac{1}{4} J_{g,smn}^- + \sum_{g'=1}^G \sum_{s'=1}^{s_M} \sum_{m'=0}^{m_M} \sum_{n'=0}^{n_M} \tilde{J}_{gg',ss'mm'nn'}^- J_{g',s'm'n'}^- \end{aligned} \quad (12)$$

The weight functions $w_{s,mn}$ are, in the present example, products of Legendre polynomials, e.g. $P_m(x)P_n(z)$ for the face 1 in Fig.1. Note that this moment method clearly overcomes (although in a somewhat brute force way) the problems due to the edges and vertices of the body V . By re-grouping the various quantities into vectors and matrices, equations (10) can be given a compact form, namely

$$\mathbf{M}^+ \mathbf{J}^+ = \mathbf{M}^- \mathbf{J}^-, \quad (13)$$

where $M_{gg',ss'mm'nn'}^\pm = \tilde{J}_{gg',ss'mm'nn'}^\pm \pm \frac{1}{4} \delta_{gg'} \delta_{ss'} \delta_{mm'} \delta_{nn'}$. After inversion of \mathbf{M}^+ , equations (13) leads to

$$\mathbf{J}^+ = \tilde{\mathbf{R}} \mathbf{J}^-, \quad (14)$$

with $\tilde{\mathbf{R}} = (\mathbf{M}^+)^{-1} \mathbf{M}^-$.

Equation (14) expresses what is usually meant as a *response matrix* approach.

The evaluation of the elements of the matrices \mathbf{M}^\pm is not easy, even for a cell with the shape of a rectangular prism. Actually, considering the interaction, so to say, of the faces 1 and 4 in Fig.??, we are led e.g. to the evaluation of the following four-fold integrals

$$I_{14,mm'nn'} = \int_0^a dx \int_0^c dz \int_0^b dy' \int_0^c dz' \frac{e^{-\gamma_h \sqrt{x^2+y'^2+(z-z')^2}}}{4\pi \sqrt{x^2+y'^2+(z-z')^2}} x^m z^n y'^{m'} z'^{n'}. \quad (15)$$

However, elementary (although very tedious) procedures, based on several integrations by parts, allow to obtain some recurrence relations which end into easy-to-compute one-dimensional integrals. Only in a few cases one must recur to a double numerical integration.

The symmetry of the cell problem (for instance, in the case of a prism with a square base) can also be exploited, in particular by means of the circulant properties of the basic matrices.

The second level of the calculation. We now give some details about the second level of the calculation. If the reactor is divided into N homogeneous cells we can write

$$\mathbf{J}^+ = \mathbf{Z}(k) \mathbf{J}^-, \quad (16)$$

where the dependence on the eigenvalue k is explicitly mentioned and the vectors \mathbf{J}^+ and \mathbf{J}^- are made of N blocks, which correspond to the outward and inward partial currents from each cell. The matrix $\mathbf{Z}(k)$ is therefore a block ($N \times N$) diagonal matrix where each block corresponds to a cell response matrix $\tilde{\mathbf{R}}$. Defining a suitable coupling matrix $\mathbf{\Pi}$ it is possible to write the partial currents entering each cell in terms of the partial currents leaving the neighbouring ones:

$$\mathbf{J}^- = \mathbf{\Pi} \mathbf{J}^+. \quad (17)$$

Thus, combining equations (17) and (16), we get

$$\mathbf{J}^+ = \mathbf{Z}(k) \mathbf{\Pi} \mathbf{J}^+ = \mathbf{\Theta}(k) \mathbf{J}^+. \quad (18)$$

This homogeneous system admits a non trivial solution only for specific values of the multiplication constant k . The following procedure can be devised in order to determine, in particular, the minimum value of k , which corresponds to the criticality constant. Let us consider the following auxiliary eigenvalue problem

$$\alpha \mathbf{J}^+ = \mathbf{\Theta}(k) \mathbf{J}^+. \quad (19)$$

We must look for the value of k that gives an α -eigenvalue equal to unity [15, 16]. This means that the J^+ 's must be invariant under the transformation (19), as expected for a steady, critical state. Thus, an iterative procedure (actually the classical power method) can be exploited to determine the α -eigenvalue for a fixed value of k :

$${}^{(n+1)}\mathbf{J}^+ = \mathbf{\Theta}(k) {}^{(n)}\mathbf{J}^+ \quad (20)$$

$${}^{(n+1)}\alpha = \left\{ \frac{\langle {}^{(n+1)}\mathbf{J}^+, {}^{(n+1)}\mathbf{J}^+ \rangle}{\langle {}^{(n)}\mathbf{J}^+, {}^{(n)}\mathbf{J}^+ \rangle} \right\}^{\frac{1}{2}}, \quad (21)$$

where equation (20) is iterated until a suitable convergence on the estimated value of ${}^{(n+1)}\alpha$, given by equation (21), is achieved. As $\alpha(k)$ turns out to be a monotonic function of k [15], the new value of k can be estimated e.g. by means of the Newton's chord method. The process will stop when a suitable convergence on the value of the multiplication constant k is obtained.

To accelerate the convergence of the above procedure, a multi-step approach was chosen: in the first step only the first moment of the partial current Legendre expansion is considered; once the convergence is achieved the procedure is then repeated considering the first two moments of the Legendre expansions and so on up to the maximum number of moments used (e.g. five). It was found that such an approach was able to cut down the computational time by a factor 20 with respect to a direct use, from the beginning of the calculation, of the maximum number of the available Legendre moments.

Finally, once the convergence over the multiplication constant k has been achieved, in order to obtain also an accurate eigenvector \mathbf{J}^+ it is necessary to perform some extra iterations according to Eq. (20), written now in the form $\mathbf{\Theta} \mathbf{J}^+ = 0$, where $\mathbf{\Theta} = \mathbf{I} - \mathbf{\Theta}(k)$. To this purpose, instead of the power method, which may result quite lengthy, an algorithm based on a Krylov subspace projection method like the Generalized Minimal RESidual algorithm (GMRES) [18] has been adopted.

The neutron transport equation. The linear Boltzmann equation (or transport equation), here again written already in a group-energy discretized form, is as follows:

$$\begin{aligned} \mathbf{\Omega} \cdot \text{grad}_{\mathbf{r}} \phi_g(\mathbf{r}, \mathbf{\Omega}) + \Sigma_{t,g}(\mathbf{r}) \phi_g(\mathbf{r}, \mathbf{\Omega}) - \sum_{g'=1}^G \int \left[\Sigma_{s,gg'}(\mathbf{r}, \mathbf{\Omega}, \mathbf{\Omega}') \right. \\ \left. + \frac{\chi_g}{k} \nu_{g'} \Sigma_{f,g'}(\mathbf{r}) \right] \phi_{g'}(\mathbf{r}, \mathbf{\Omega}') d\mathbf{\Omega}' = 0 \quad (g = 1, \dots, G). \end{aligned} \quad (22)$$

The (capital) improvement obtained by solving this equation, as compare with the much less accurate diffusion approach, is due by the intervention of the supplementary angular variable $\mathbf{\Omega}$, representing the direction of the particle beams in which the neutron field can be subdivided, indeed an important deepening of the description of the physical process.

The variable $\mathbf{\Omega}$ can be discretized or, in a more elegant form, the fluxes $\phi_g(\mathbf{r}, \mathbf{\Omega})$ can be expanded in terms of spherical harmonics $Y_{lm}(\mathbf{\Omega})$ (or $Y_{lm}(\theta, \varphi)$, with the usual notation), as well as the kernels $\Sigma_{s,gg'}(\mathbf{r}, \mathbf{\Omega}, \mathbf{\Omega}')$.

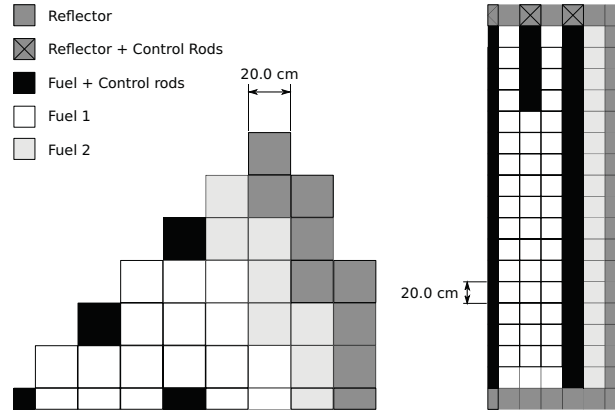


Figure 2: Geometrical configuration and material composition of the IAEA 3D benchmark problem.

For plane-parallel problems (\mathbf{r} is then simply replaced by x) the spherical harmonics reduce to the Legendre polynomials and it is not difficult to show that the system so obtained has the form of a system of (ordinary) linear differential equations of the first order or also, after suitable manipulations, of the second order.

In the general 3D case, even for a moderate value of the order L of the differential spherical harmonics equation system turns out to be overwhelming. A successful, although rude, idea in order to simplify the matter is to ignore the dependence on the azimuthal angle φ . Then it is again possible to arrive at a system of 3D diffusion equations (their number is now $L \times G$) to which BEM can still be applied [19, 20, 21, 22]. The example in the next section illustrates the improvement obtainable by such simplified spherical harmonics method with respect to the diffusion method.

Numerical examples The first numerical example is a transport version prepared by Hébert [23] of the classical IAEA 3D benchmark problem of the Argonne Code Center [24] (see Fig.2). As stated by the author, the original cross section data have been converted in order to allow transport-like calculations consistent with the diffusion theory results. The IAEA 3D benchmark concerns a full 3D simplified version of a typical LWR core, where nine assemblies have fully inserted control rods while four assemblies have partially inserted control rods. The active part of the reactor core is made of 17 layers, 20 cm high. The four control rods partially inserted are dipped from the top of the active core by 80 cm. Finally, a reflector layer, 20 cm high, is present at the top and the bottom of the reactor core. A vacuum boundary condition is adopted on the external surface of the lateral and axial reflector. The values of the multiplication constant obtained with the diffusion and SP3 (Simplified spherical harmonics with order $N=3$) approximations through the Boundary Element - Response Matrix (BERM) method are compared in Table 1 with the reference value obtained by a suitable two energy group MCNP Monte Carlo calculation [25].

The second example is derived from a benchmark problem [26] concerning the calculation of a 3D reactor core made of 16 fuel assemblies (quarter core symmetry), half of which contain mixed-oxide (MOX) fuel rods, and completely surrounded by a water reflector (see Fig.3). In the present case the number of mixed oxide mixtures has been reduced from three to one. Each fuel assembly is made of 17×17 square pin cells the side length of which is 1.26 cm. In this application, each pin cell has been spatially homogenized weighting the cross section over the volumes, with a preliminary estimate of the neutron flux within each cell. The sets of cross sections so obtained are reported in [21, Appendix B]. There are control rods inserted $2/3$ of the way into the inner UO_2 assembly and $1/3$ of the way

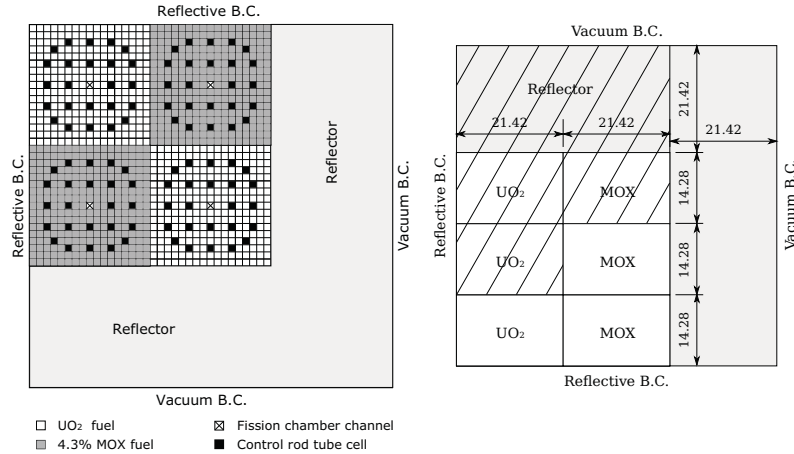


Figure 3: Horizontal (left) and vertical (right) sections of the 3D MOX reactor core (dimensions are in cm). In the present configuration the control rods are crossing the upper reflector and inserted by 2/3 of the way into the inner UO₂ fuel assembly and 1/3 of the way into the two MOX fuel assemblies (hatched region).

into both MOX assemblies, as indicated by the hatched region in Fig. 3. Finally, a vacuum boundary condition is applied on the external surface of the reflector and, in order to reduce the computational burden, an axial symmetry is also assumed.

In order to define the reference multiplication constant, again a suitable MCNP Monte Carlo calculation was run making use of the same sets of cross sections used by the deterministic code.

Table 1: The multiplication constant k for the transport version of the IAEA 3D benchmark.

Code	k	Δk (pcm)
MCNP6 ^a (ref.)	1.02955	—
BERM-diffusion	1.02907	-48
BERM-SP3	1.02956	1

^a with an estimated standard deviation of ± 0.00002 .

Table 2: The multiplication constant k for the 3D MOX reactor core.

Code	k	Δk (pcm)
MCNP6 ^a (ref.)	1.05932	—
BERM-SP3	1.05755	-177
BERM-SP7	1.05838	-94

^a with an estimated standard deviation of ± 0.00004 .

Table 2 compares the reference value of the multiplication constant with those obtained by two BERM calculations in the SP3 and SP7 transport approximations (i.e. Simplified Spherical Harmonics with order $N=3$ and $N=7$, respectively). No results obtained with the diffusion approximation are shown for this example because, due to the too small size of the computational cells, they turned out to be rather inaccurate, as expected.

Conclusions The present paper shows an application to nuclear reactor cores of the Boundary Element method associated with a Response Matrix approach. The calculation efficiency is improved by the use of suitable recurrence formulas for the evaluation of the boundary integrals and by other

acceleration techniques to determine the neutron flux distribution in the core and the criticality constant. Results show that the method is very accurate and represents a good alternative to the usual Finite Element methods.

References

- [1] Koskinen, H. (1965) In UN, (ed.), Proceedings of the 3rd International Conference on the Peaceful Uses of Atomic Energy, Geneva, volume 4, : pp. 67–73.
- [2] Itagaki, M. (1985) *Journal of Nuclear Science and Technology* **22(7)**, 565–583.
- [3] Itagaki, M. and Brebbia, C. A. (1991) *Nuclear Science Engineering* **107(3)**, 246 – 264.
- [4] Novak A.J. and Neves A.C., (ed.) The multiple reciprocity boundary element method chapter 6 Computational Mechanics Publications, Southampton (1994).
- [5] Itagaki, M. (1995) *Engineering Analysis with Boundary Elements* **15(3)**, 289 – 293.
- [6] Itagaki, M. (2000) *Engineering Analysis with Boundary Elements* **24(2)**, 169 – 176.
- [7] Itagaki, M. (2002) *Engineering Analysis with Boundary Elements* **26(9)**, 807 – 812.
- [8] Ozgener, B. (1998) *Annals of Nuclear Energy* **25(6)**, 347–357.
- [9] Ozgener, B. and Ozgener, H. (2000) *Engineering Analysis with Boundary Elements* **24(3)**, 259–269.
- [10] Cavdar, S. and Ozgener, H. A. (2004) *Annals of Nuclear Energy* **31(14)**, 1555 – 1582.
- [11] Purwadi, M. D., Tsuji, M., Narita, M., and Itagaki, M. (1997) *Engineering Analysis with Boundary Elements* **20(3)**, 197 – 204.
- [12] Purwadi, M. D., Tsuji, M., Narita, M., and Itagaki, M. (1998) *Nuclear Science and Engineering* **129(1)**, 88–96.
- [13] Chiba, G., Tsuji, M., and Shimazu, Y. (2001) *Journal of Nuclear Science and Technology* **38(8)**, 664–673.
- [14] Chiba, G., Tsuji, M., and Shimazu, Y. (2001) *Annals of Nuclear Energy* **28(9)**, 895–912.
- [15] Maiani, M. and Montagnini, B. (1999) *Annals of Nuclear Energy* **26(15)**, 1341 – 1369.
- [16] Maiani, M. and Montagnini, B. (2004) *Annals of Nuclear Energy* **31(13)**, 1447 – 1475.
- [17] Cossa, G., Giusti, V., and Montagnini, B. (2010) *Annals of Nuclear Energy* **37(7)**, 953–973.
- [18] Saad, Y. and Schultz, M. H. (1986) *SIAM Journal of Scientific and Statistical Computing* **7(3)**, 856–869.
- [19] Larsen, E. W., Morel, J. E., and McGhee, J. M. (1996) *Nuclear Science Engineering* **123**, 328 – 342.
- [20] McClarren, R. G. (2011) *Transport Theory and Statistical Physics* **39(2-4)**, 73–109.
- [21] Giusti, V. and Montagnini, B. (2012) *Annals of Nuclear Energy* **42**, 119–130.
- [22] Giusti, V., Montagnini, B., and Ravetto, P. (2013) *Annals of Nuclear Energy* **57**, 350–367.
- [23] Hébert, A. (2010) *Annals of Nuclear Energy* **37(4)**, 498 – 511.
- [24] ANL-7416 (1977) Benchmark Problem Book, Supplement 2, Argonne National Laboratory, Argonne IL, USA.
- [25] Pelowitz D.B. (Ed.) MCNP6 User’s Manual, Ver.1 LA-CP-13-00634 Los Alamos National Laboratory (2013).
- [26] Smith, M. A., Lewis, E. E., and Na, B.-C. Benchmark on Deterministic Transport Calculations Without Spatial Homogenisation NEA/NSC/DOC(2005)16 OECD Nuclear Energy Agency (2005).